X-ray absorption spectroscopy of detwinned PrxY1-xBa2Cu3O7-y single crystals: electronic structure and hole distribution

Merz, M.; Nücker, N.; Pellegrin, E.; Schweiss, P.; Schuppler, S.; Kielwein, M.; Knupfer, M.; Golden, M.S.; Fink, J.

Published in:
Physical Review. B, Condensed Matter

DOI:
10.1103/PhysRevB.55.9160

X-ray absorption spectroscopy of detwinned $Pr_xY_{1-x}Ba_2Cu_3O_{7-y}$ single crystals: Electronic structure and hole distribution

M. Merz, N. Nücker, E. Pellegrin,* P. Schweiss, and S. Schuppler
Forschungszentrum Karlsruhe, INFP, P.O. Box 3640, D-76021 Karlsruhe, Germany

M. Kielwein, M. Knupfer, M. S. Golden, and J. Fink
Institut für Festkörper- und Werkstofforschung Dresden, P.O. Box 270016, D-01171 Dresden, Germany

C. T. Chen
Synchrotron Radiation Research Center, Hsinchu Science-based Industrial Park, Hsinchu 300, Taiwan

V. Chakarian and Y. U. Idzerda
Naval Research Laboratory, Code 6345, Washington, D.C. 20375

A. Erb
Département de Physique de la Matière Condensée, Université de Genève, 24, quai Ernest-Ansermet, CH-1211 Genève, Switzerland
(Received 22 August 1996)

Substituting Y in orthorhombic $(Y,R)Ba_2Cu_3O_7$ by any rare-earth element R has generally little effect on the superconducting properties. For R=Pr, however, superconductivity is completely suppressed. To understand this effect we have studied the unoccupied electronic structure of $Pr_xY_{1-x}Ba_2Cu_3O_{7-y}$ ($x=0.0,\ 0.4,\ 0.8$) using polarization-dependent O 1s near-edge x-ray absorption spectroscopy of detwinned single crystals. We identify the hole states in the CuO_2 planes and the CuO_3 chains and give estimates of the relative contributions of the O $2p_x$, O $2p_y$, and O $2p_z$ orbitals to these states. Along with the comparison of oxygen-rich ($y\approx0.1$) to the oxygen-depleted materials ($y\approx0.9$), this allows a test of the current theoretical explanations for the Pr-induced suppression of superconductivity. While we can rule out models involving hole filling or charge transfer between the planes and the chains, our data are consistent with approaches based on Pr $4f$–O $2p_\pi$ hybridization. [S0163-1829(97)03313-4]

I. INTRODUCTION

The discovery of high-temperature superconductivity (HTSC) in 1986 (Ref. 1) has triggered a cascade of theoretical and experimental research concerning the underlying mechanism of HTSC, but nevertheless an unambiguous answer to the question of the origin of HTSC remains elusive. Much work has concentrated on direct determinations of the spatial, electronic, and phonon structure of high-temperature superconductors. One complementary approach is to investigate compounds obtained from high-temperature superconductors by specifically substituting characteristic elements, thereby reducing or even suppressing the superconducting transition temperature T_c. A most interesting example exists within the family related to $YBa_2Cu_3O_{7-y}$,[2] where the suppression of superconductivity upon replacing Y with Pr has generated a lively discussion in recent years.

The crystallographic structure of the $RBa_2Cu_3O_{7-y}$ compounds (R denotes Y and rare earths) is based on a modified perovskite template containing two-dimensional CuO_2 planes and one-dimensional CuO_3 chains embedded between Ba and R layers as shown in Fig. 1. (In the case of $TbBa_2Cu_3O_{7-y}$ and $CeBa_2Cu_3O_{7-y}$ the orthorhombic 1-2-3 structure could not be synthesized.) For $YBa_2Cu_3O_{7-y}$ it has been suggested that the block layers act as a charge reservoir and that due to their interaction with adjacent CuO_2 planes they are able to supply holes for the planes when the CuO_3 chains are formed. Since almost all isostructural members of the rare-earth-based 1-2-3 family result in a high-temperature superconductor with transition temperature near 93 K,[3–5] it was assumed that the rare-earth atoms serve merely as counterions stabilizing the structure without significantly affecting the superconducting properties. Among those rare-earth-based cuprates that are isostructural to $YBa_2Cu_3O_{7-y}$, the $PrBa_2Cu_3O_{7-y}$ compound is a puzzling exception since it shows neither metallic nor superconducting behavior.[6–10] Upon substituting Pr into the $Pr_xY_{1-x}Ba_2Cu_3O_{7-y}$ system, T_c decreases[11–13] and, in the case of $y\approx0.1$, finally vanishes for Pr fractions x beyond 0.55. This transition seems to be accompanied by a change from metallic to semiconducting characteristics.[10,12,14] Concurrently, an antiferromagnetic order of the copper atoms in the planes[15–18] and of the Pr atoms between the planes[15,16,18] sets in, resulting in Néel temperatures $T_{N,\mathrm{Cu(2)}}\approx285$ K and $T_{N,\mathrm{Pr}}\approx 17$ K for the fully Pr-substituted compound ($x=1$). Since $PrBa_2Cu_3O_{7-y}$ has all the structural features that are considered essential for high-temperature superconductivity in $YBa_2Cu_3O_{7-y}$, such as CuO_2 planes and CuO_3 chains which lead to a doping of the planes, differences in the electronic structure and in the hole distribution between these structural units may reveal key parameters for high-temperature superconductivity in $RBa_2Cu_3O_{7-y}$ and, therefore, might help to close in on the mechanism that underlies superconductivity.

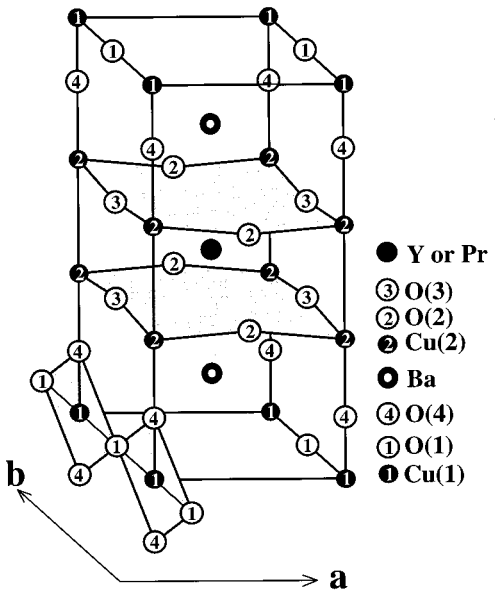

FIG. 1. The unit cell of $Pr_xY_{1-x}Ba_2Cu_3O_7$. The CuO_2 planes and the CuO_3 chains are emphasized by a gray shading. The Pr atom substitutes directly on the Y site in the center of the unit cell.

In order to explain the T_c suppression in the p-type system $Pr_xY_{1-x}Ba_2Cu_3O_{7-y}$, up to now several models have been suggested while still no general agreement on the Pr valence has been reached. The prevailing proposals can be divided into three main categories: (i) filling of mobile holes, (ii) magnetic interaction and/or localization effects mediated through hybridization of Pr $4f$ with O $2p$ states, and (iii) gradual hole transfer between the planes and the chains.

(i) In the hole-filling model the Pr valence is assumed to be greater than $+3$ to explain the lack of metallic behavior in $PrBa_2Cu_3O_7$ and also to account for the Ca-induced recovery of superconductivity in thin films of $Pr_{0.5}Ca_{0.5}Ba_2Cu_3O_7$.[19] Since superconductivity in $YBa_2Cu_3O_{7-y}$, just as in $La_{2-x}Sr_xCu_2O_{4+\delta}$, requires holes in the conducting CuO_2 planes,[20,21] delocalized holes in the planes are annihilated due to the substitution of trivalent Y by Pr with a valence greater than $3+$. This approach implies that the suppression of superconductivity results from a reduced number of charge carriers in the CuO_2 planes. Magnetic susceptibility,[6,8,12] Hall effect,[8] thermopower,[7,9,10] nuclear magnetic resonance,[15] muon-spin relaxation,[16] and neutron diffraction measurements[22–24] have been interpreted in terms of hole depletion. On closer inspection, however, it has been shown that these results can also be understood as an indication for Pr^{3+}. For example, Sø derholm *et al.*[25] and Hilscher *et al.*[26] were able to explain the reduced magnetic moment, taking a crystal field splitting of the $^3H_4$ ground state of Pr^{3+} into consideration. On the other hand, most band structure calculations[27] and high-energy spectroscopy experiments support a trivalent Pr atom. These experiments include resonant photoemission spectroscopy,[28] x-ray absorption,[29,30] and electron energy-loss spectroscopy[31] on the O $1s$, Pr $2p$, and Pr $3d$ edges. Taken together, this evidence effectively rules out hole filling as responsible for the lack of superconductivity.

(ii) Alternatively, a magnetic pair-breaking effect by the local moment of the Pr atom has been invoked as an explanation,[12,27] since the degradation of T_c with increasing Pr concentration seemed to be compatible with Abrikosov-Gorkov theory. However, pair breaking itself does not localize charge carriers and, thus, explains neither the nonmetallicity in $PrBa_2Cu_3O_7$ nor the recovery of superconductivity upon doping with Ca. In addition, T_c remains wholly unaffected upon substitution of Y by Gd although the Gd $^8S_{7/2}$ ground state exhibits a much stronger magnetic moment than the $^3H_4$ ground state of Pr^{3+}.

Quite early on, a further approach to this problem was put forward: O $2p_\sigma$ holes (for nomenclature see Ref. 34) are still present in the CuO_2 planes but are assumed to be strongly hybridized with Pr $4f$ states.[31] This renders the initially mobile holes localized and in effect leads to the insulating and nonsuperconducting behavior observed. However, this explanation was also refuted as hybridization of Pr $4f$ with O $2p_\sigma$ states vanishes by symmetry and the hybridization with Cu $3d_{x^2-y^2}$ states is very small. Thus, based on the optical data of Takenaka *et al.*,[32] Fehrenbacher and Rice (FR) explained the absence of superconductivity in $PrBa_2Cu_3O_7$ by the existence of a local Pr $4f_{z(x^2-y^2)}$–O $2p_\pi$ hybridized state[33,34] which binds the holes of the planes to Pr sites. They conclude that holes are transferred from primarily planar O $2p_\sigma$ to O $2p_\pi$ orbitals, i.e., from the Zhang-Rice (ZR) state[35,36] into this FR state. According to Fehrenbacher and Rice, the only possible hole state is a superposition of the eight O(2,3) $2p_\pi$ orbitals with $f_{z(x^2-y^2)}$ symmetry with respect to the central Pr atom, and they assume that the O $2p_\pi$ orbitals point towards the Pr atom. This seems to suggest that the O $2p_\pi$ orbitals are ''rotated'' by about 45° with respect to the CuO_2 planes.[33,34] To facilitate the hybridization between the eight O $2p_\pi$ orbitals and the $f_{z(x^2-y^2)}$ states of the central Pr atom a fraction $n_F \approx 0.5$ of all Pr atoms has to be in the formal oxidation state IV. Finally, Fehrenbacher and Rice assess the number of holes transferred to the Pr atom to be $n_{Pr} \approx 0.15$–0.2. Remarkably, this small number—still compatible with the experimental findings for the Pr valence—suffices to stabilize the FR hybridization, thus localizing the holes in the Pr $4f_{z(x^2-y^2)}$–O $2p_\pi$ orbitals.

Taking correlation effects on the rare-earth site into account, Liechtenstein and Mazin presented local density approximation (LDA)$+U_{Pr}$ calculations based on the idea of FR states.[37] In contrast to Fehrenbacher and Rice,[33] they find a dispersive ligand band in place of local p_π orbitals with $f_{z(x^2-y^2)}$ symmetry around the central R atom. Due to the interaction with the Pr $4f$ state, the top of this ligand band is partially pushed above the Fermi level, thereby grabbing the mobile holes from the ZR state. Liechtenstein and Mazin emphasize that this band has mainly planar character at the zone corner, where the band is above the Fermi level (E_F), and p_z character only at the zone center, where the FR band lies ≈ 2 eV below E_F. In order to account for the insulating behavior of $PrBa_2Cu_3O_7$ they assume substantial disorder on the Pr site.

(iii) A further model based on the Hamiltonian of Fehrenbacher and Rice was proposed by Wang *et al.*[38] In their approach, three states are competing close to the Fermi level: the ZR state, the FR state, and the hole states of the CuO_3 chains. Upon increasing the Pr concentration to $x=0.5$ all of the holes residing on the ZR state are transferred to the FR state. On further Pr doping, chain holes, too, are transferred

to the FR state and, finally, for $PrBa_2Cu_3O_7$ all holes reside on the FR state and none are left in the chains.

A qualitative discussion of the electronic structure of $Pr_xY_{1-x}Ba_2Cu_3O_7$ was given by Khomskii.[39] He proposed a gradual charge redistribution between planes and chains upon increasing Pr content. Therefore, beyond a critical Pr concentration all the remaining holes should reside on the chains—predominantly on the O(1) $2p_y$ orbitals—and no holes should be left in the planes.

Lately, Blackstead and Dow suggested a model which is based on disorder effects on the Ba site.[40] They argue that, while superconductivity is still present in the chains of ideal $PrBa_2Cu_3O_7$, it is quenched in real crystals by magnetic pair breaking due to Pr impurities on the Ba sites.

The aim of this paper is to distinguish between the various models by carefully examining the electronic structure of $PrBa_2Cu_3O_{7-y}$ close to the Fermi level. For this, we have conducted O 1*s* near-edge x-ray absorption fine structure (NEXAFS) studies of $Pr_xY_{1-x}Ba_2Cu_3O_{7-y}$. Utilizing the linearly polarized character of synchrotron radiation we took a critical look at the various models mentioned above. In particular, if FR states do exist, NEXAFS should be well suited for determining a rotation angle[34] of the O(2,3) $2p_\pi$ orbitals.

The paper is organized as follows: Section II covers sample preparation and data collection. In Sec. III, we will expound the features of the NEXAFS data after briefly reviewing the results of our neutron diffraction mesurements. Section IV discusses the implications of the NEXAFS results and, finally, the conclusions are drawn in Sec. V.

II. EXPERIMENT

$Pr_xY_{1-x}Ba_2Cu_3O_{7-y}$ single crystals were grown using standard methods. Full details of the growth process can be found in Refs. 41 and 42. The use of Al_2O_3 crucibles was avoided since they introduce Al impurities of up to 50% on the Cu(1) sites.[42] For $x=0.0$ and 0.8, the samples were grown in an Y_2O_3-stabilized ZrO_2 crucible, which resulted in crystals with no detectable Zr content. The $Pr_{0.4}Y_{0.6}Ba_2Cu_3O_{7-y}$ crystals were grown in a novel inert $BaZrO_3$ crucible.[42] Crystals with $x=0.0$ and 0.8 from the same batches were characterized by energy-dispersive x-ray emission (EDX) and neutron diffraction (see below) for impurities, stoichiometry, and structural parameters. The oxygen content $7-y$ of $Pr_xY_{1-x}Ba_2Cu_3O_{7-y}$ ($x=0.8$, 0.0) was determined to be 6.91 ± 0.01. Since the $Pr_{0.4}Y_{0.6}Ba_2Cu_3O_{7-y}$ crystals were oxygenated by the same method as the $x=0.8$ and 0.0 crystals, we expect the oxygen content of the former to also be 6.91. Whereas for $x=0.0$ we find no oxygen on the O(5) site, for $x=0.8$ an occupancy of up to 5% cannot be excluded from the refinements of the neutron diffraction data.

Oxygen-deficient samples were obtained by annealing as-grown crystals of the same batch at 650 °C in a vacuum of about 10^{-9} mbar for several days. Subsequently, the oxygen content $7-y$ was checked with optical reflectivity measurements and was estimated to be 6.05 for $Pr_{0.8}Y_{0.2}Ba_2Cu_3O_{7-y}$ and 6.15 for $YBa_2Cu_3O_{7-y}$.[43] The oxygen-loaded $Pr_xY_{1-x}Ba_2Cu_3O_{7-y}$ crystals were detwinned in a process similar to the one for $YBa_2Cu_3O_{7-y}$, which is discussed in detail elsewhere.[41,42,44] Well-reflecting flat (001) surfaces of the samples were obtained by cutting off the crystals' top layers using the diamond knife of an ultramicrotome.

The neutron diffraction experiments were performed on larger, twinned crystals from the same batches at the four-circle diffractometer 5C2 at the Orphée reactor, Laboratoire Léon Brillouin, CE Saclay.[45] Experimental details, like scan range adjustment in order to achieve a complete integration over the typical multipeak structure of the twinned crystals, background, absorption, and extinction treatments, are discussed in Ref. 46. For the structure refinement we used the PROMETHEUS program package in a version for data sets obtained for twinned crystals.[47] The twinning leads to correlations between some u_{11} and u_{22} mean-square displacements, which were taken into consideration by introducing constraints.

The O 1*s* absorption spectra[48] were obtained using linearly polarized synchrotron radiation from beamline U4B at the National Synchrotron Light Source (NSLS), Brookhaven National Laboratory. For moderate photon energies and a small extension of the core level transitions obeying dipole selection rules dominate, and higher-order transitions can be neglected. Applying dipole selection rules, the unoccupied part of the O $2p$ final states can be reached from the initial O 1*s* core level. Therefore, polarization-dependent NEXAFS measurements on detwinned single crystals provide insight into the symmetry of the hole states at E_F and, thus, enable an estimate of the relative hole distribution between the different O sites in the crystal structure. The latter is possible if the binding energies for the various oxygen sites are taken into account. In the setup used, a multielement Ge fluorescence detector was placed at an angle of 55° with respect to the incoming photon beam. The samples were mounted on a manipulator allowing rotation around the horizontal and vertical axes. The in-plane spectra ($\mathbf{E}\|a$ and $\mathbf{E}\|b$) were obtained in a normal-incidence alignment. To fully explore and separate out the orbital character and symmetry of the hole states in the CuO_2 planes, the measurements are best performed for many different azimuthal sample orientations relative to the polarization vector of the incoming light. Such a series of angle-dependent measurements allows the correction of in-plane misalignment. In order to reach out-of-plane orbitals, the samples were rotated to achieve angles of incidence of 15°, 30°, 45°, 65°, and 80° with respect to the surface normal (grazing incidence). Such measurements are indispensible to ensure that the light hits neither parts of the sample holder nor the conducting glue. Furthermore, corrections for polar misalignment are possible if grazing incidence measurements are carried out at many different angles. According to

$$I(\theta)=I_{\|c}\cos^2(\theta)+I_{\perp c}\sin^2(\theta), \tag{1}$$

the $\mathbf{E}\|c$ spectra were calculated by correcting for the corresponding angle of incidence. The correction of spectra taken at polar incidence angles of 45°, 65°, and 80° led to nearly identical results.

Since the probing depths for total electron yield and fluorescence yield (FY) in the actual setup were approximately 50 and 600 Å, respectively, we have recorded the NEXAFS

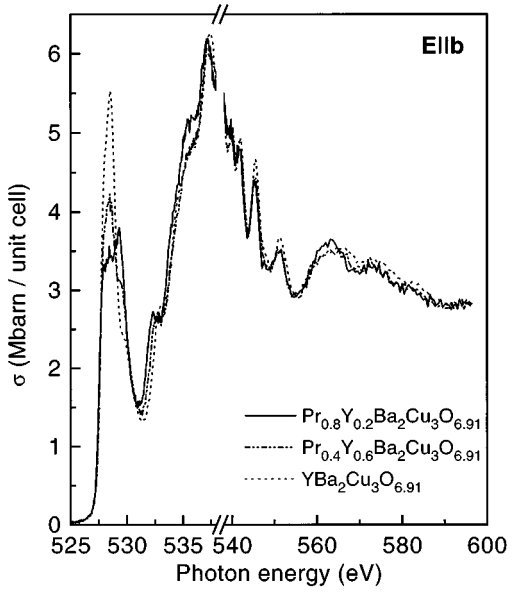

FIG. 2. O 1*s* absorption spectra of $Pr_{0.8}Y_{0.2}Ba_2Cu_3O_{6.91}$, $Pr_{0.4}Y_{0.6}Ba_2Cu_3O_{6.91}$, and $YBa_2Cu_3O_{6.91}$ for polarization $\mathbf{E}\|b$. The data are shown in the entire energy range recorded. Above 540 eV, the cross sections are independent of the Pr concentration.

spectra in the FY detection mode to obtain information about the bulk properties and to avoid problems associated with surface sensitivity. However, FY spectra are affected by saturation and self-absorption effects which cannot be ignored.[49,50] The incoming photon intensity is attenuated not only by the oxygen absorption coefficient $\mu_{\mathrm{oxy}}(E)$, but also by the absorption coefficient $\mu_{\mathrm{bac}}(E)$, of all the other elements in the sample. The radiative filling of the O 1*s* core hole after the absorption process results in the emission of fluorescence radiation. The intensity of this emission process is proportional to $\mu_{\mathrm{oxy}}(E)$. On their way to the sample surface the fluorescence x rays are attenuated by the total absorption coefficient $\mu_{\mathrm{tot}}(E_f)=\mu_{\mathrm{oxy}}(E_f)+\mu_{\mathrm{bac}}(E_f)$ at the energy of the fluorescence radiation, E_f. A simple calculation shows that the normalized fluorescence intensity μ_{FY} is given by the relation

$$\mu_{\mathrm{FY}}\equiv\frac{I_f(E)}{I_0(E)}\propto\frac{\mu_{\mathrm{oxy}}(E)}{\mu_{\mathrm{tot}}(E)/\cos\alpha+\mu_{\mathrm{tot}}(E_f)/\cos\beta},\qquad(2)$$

where $I_f(E)$ is the intensity of the fluorescence radiation detected, $I_0(E)$ the primary intensity, α the angle between the incoming beam and the sample normal, and β the angle between the sample normal and the outgoing beam. In the limit of dilute samples the contribution of $\mu_{\mathrm{oxy}}(E)$ to $\mu_{\mathrm{tot}}(E)$ is very small and, therefore, $\mu_{\mathrm{FY}}(E)\propto\mu_{\mathrm{oxy}}(E)$. For $Pr_xY_{1-x}Ba_2Cu_3O_{7-y}$ this is not the case, and we have corrected our data for these effects. The spectra were normalized to the tabulated standard absorption cross section[51,52] in the energy range 590 eV $\leqslant E \leqslant$ 600 eV. In this range the spectra are almost structureless and the atomiclike spectral weight is only slightly modified by EXAFS effects as shown for the $\mathbf{E}\|b$ spectra in Fig. 2, which is representative for all polarizations. The energy resolution in our measurements was about 220 meV at an incident photon energy of 530 eV and the degree of linear polarization was estimated to be (97 $\pm$1)% for the experimental configuration used.

TABLE I. Structural parameters of $Pr_xY_{1-x}Ba_2Cu_3O_{6.91}$ determined by neutron diffraction on single crystals. See Fig. 1 for positional notation. The u_{ii} denote the mean-square displacements along the principal axes, z the atomic position in the c direction, and a, b, and c the lattice parameters.

		$x=0.8$	$x=0.0$
	a (Å)	3.868(5)	3.819(8)
	b (Å)	3.926(5)	3.884(8)
	c (Å)	11.708(17)	11.681(31)
RE	u_{11} (Å^2)	0.0039(5)	0.0051(2)
	u_{33} (Å^2)	0.0048(6)	0.0050(4)
Ba	z	0.18213(8)	0.18505(10)
	u_{11} (Å^2)	0.0085(3)	0.0076(2)
	u_{33} (Å^2)	0.0081(4)	0.0075(4)
Cu(1)	u_{11} (Å^2)	0.0094(3)	0.0075(4)
	u_{33} (Å^2)	0.0055(4)	0.0048(5)
Cu(2)	z	0.35119(6)	0.35576(7)
	u_{11} (Å^2)	0.0041(2)	0.0036(2)
	u_{33} (Å^2)	0.0079(2)	0.0075(3)
O(1)	u_{11} (Å^2)	0.0252(9)	0.0273(15)
	u_{22} (Å^2)	0.0098(10)	0.0078(11)
	u_{33} (Å^2)	0.0115(9)	0.0124(10)
O(2)	z	0.37409(8)	0.37872(22)
	u_{11} (Å^2)	0.0051(2)	0.0050(2)
	u_{22} (Å^2)	0.0088(2)	0.0064(2)
	u_{33} (Å^2)	0.0115(8)	0.0100(9)
O(3)	z	0.37316(8)	0.37781(8)
	u_{11} (Å^2)	0.0088(2)	0.0064(2)
	u_{22} (Å^2)	0.0051(2)	0.0050(2)
	u_{33} (Å^2)	0.0111(8)	0.0100(9)
O(4)	z	0.15793(8)	0.15801(9)
	u_{11} (Å^2)	0.0158(4)	0.0122(4)
	u_{33} (Å^2)	0.0076(4)	0.0076(4)

III. RESULTS

Before addressing our NEXAFS results in the main body of this section, we first evaluate the structural information obtained from neutron diffraction: An important result is that there is no indication for any Pr situated on the Ba position and any Ba situated on the Pr position in our $Pr_{0.8}Y_{0.2}Ba_2Cu_3O_{7-y}$ single crystals. This follows from two observations: First, the Ba atom is too large to occupy a *R* site. Second, the Pr concentration revealed by EDX, 0.77, is in excellent agreement with the neutron data if for the refinements Pr on Ba sites is excluded and only Pr at Y sites is taken into account. Therefore, in contrast to the models of Refs. 37 and 40, neither Pr atoms on the Ba site nor Ba atoms on the Pr site are consistent with our results. The structural parameters obtained from neutron diffraction measurements are listed in Table I. The results of the present investigation are in good agreement with previously published neutron diffraction studies on powder samples.[22,23] Compared to $YBa_2Cu_3O_{7-y}$, a shrinkage of the Cu(2)-O(4) bond length is evident from our data while the Cu(2)-O(2,3)

and also the Cu(2)-Cu(2) distances are enlarged due to the substitution of Y by Pr. The Cu(1)-O(4) bond length remains almost unchanged by the substitution whereas the *R*-O(2,3) distances are strongly enhanced. Compared with other rare-earth substitutions, however, the anisotropy between the *R*-O(2) and the *R*-O(3) distances is anomalously reduced.[23] Thus, if Y is substituted by Pr, the CuO_2 planes are pushed towards the Ba-O(4) layers due to the larger radius of the rare-earth ion. Since the ionic radius of Pr^{4+} is smaller than the one of Y^{3+}, this is possible only if most of the Pr atoms are trivalent. Of course, it cannot be excluded that some Pr^{4+} is present. We will further dwell on this point in Sec. IV where we discuss the hole distribution in $Pr_xY_{1-x}Ba_2Cu_3O_{7-y}$.

Figure 2 shows the O 1*s* absorption spectra of $Pr_xY_{1-x}Ba_2Cu_3O_{6.91}$ ($x=0.0$, 0.4, 0.8) in the entire photon energy range recorded (525 eV $\leqslant E \leqslant$ 600 eV), with the electric field vector **E** adjusted parallel to the *b* axis of the crystals. These $\mathbf{E}\|b$ spectra are shown as representatives for all polarizations. They were corrected for the intensity variations of the monochromatized synchrotron radiation I_0 as well as for self-absorption and saturation effects, and normalized to the standard absorption cross section as outlined above. Beyond 535 eV, the spectra of the three crystals exhibit only small differences. From 540 eV on, they become virtually indistinguishable within statistics. The hybridized oxygen states situated in the energy range around 535 eV are not altered by Pr substitution. Thus, these features may be assigned to hybridization of oxygen with Cu (4*s*, 4*p*, ...) or Ba states. The latter would also be consistent with the Ba-O bond lengths (Table I), which are only slightly affected by the substitution. Stronger changes in the absorption spectra are observed in the vicinity of the Fermi level. Hence, the following spectra are shown in the energy range between 525 eV and 535 eV.

In Figs. 3 and 4, the O 1*s* absorption edges with polarization $\mathbf{E}\|a$ and $\mathbf{E}\|b$, respectively, are shown for the antiferromagnetic insulator $Pr_{0.8}Y_{0.2}Ba_2Cu_3O_{6.91}$, the *p*-type-doped superconductor $YBa_2Cu_3O_{6.91}$ ($T_c \approx 93$ K), and the $Pr_{0.4}Y_{0.6}Ba_2Cu_3O_{6.91}$ sample. The latter compound is still metallic and exhibits a $T_c \leqslant 15$ K. Below 534 eV the $\mathbf{E}\|a$ spectra of the three crystals (see Fig. 3) are composed of three main peaks (marked by arrows). The first peak at 528.5 eV shows a strong intensity reduction with increasing Pr concentration whereas the second and third features at 529.5 eV and 532.2 eV are strongly increased. For the Pr-doped samples the last of these three peaks appears somewhat broader than the other features and extends from about 531.5 eV to 533 eV. A further, smaller peak, independent of the Pr substitution, is seen at 530.7 eV. The feature at 528.5 eV which is most pronounced for $YBa_2Cu_3O_{6.91}$ has a width of $\Delta E \approx 1.2$ eV and a steeper onset than the following features. In accordance with previous work, this feature is attributed to ZR states.[35,36] The steep onset for $YBa_2Cu_3O_{6.91}$ indicates that the Fermi level appears to be located below the top of this ZR band. From x-ray photoemission spectroscopy (XPS) measurements[53] on the $Pr_xY_{1-x}Ba_2Cu_3O_{6.91}$ system it appears that the binding energies of the O atoms are independent of the Pr concentration. With these XPS results, the downward shift of the second peak observed in Fig. 3 leads to the conclusion that with

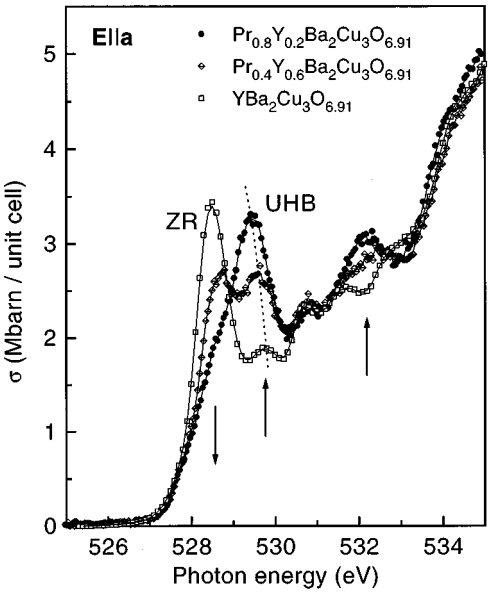

FIG. 3. Comparison of the O 1*s* absorption spectra of $Pr_{0.8}Y_{0.2}Ba_2Cu_3O_{6.91}$, $Pr_{0.4}Y_{0.6}Ba_2Cu_3O_{6.91}$, and $YBa_2Cu_3O_{6.91}$ for $\mathbf{E}\|a$. Upon Pr substitution, the upper Hubbard band increases strongly at the expense of the ZR state.

increasing Pr content the Fermi level together with the O 1*s* core level is shifted to higher energies. Finally, for $Pr_{0.8}Y_{0.2}Ba_2Cu_3O_{6.91}$ E_F is located slightly above the upper edge of the ZR band and no doped holes are left in O(2,3) 2 $p_{x,y}$ σ orbitals hybridized with Cu(2) $3d_{x^2-y^2}$ orbitals. An analogous trend as for $\mathbf{E}\|a$ is observed in Fig. 4 for the polarization $\mathbf{E}\|b$ with the main difference that for all samples the peak at 532.5 eV is not as distinct as for $\mathbf{E}\|a$ but instead a broad shoulder between 531.5 eV and 533 eV is seen.

Neglecting unoccupied π-bonded O orbitals, $\mathbf{E}\|a$ contri-

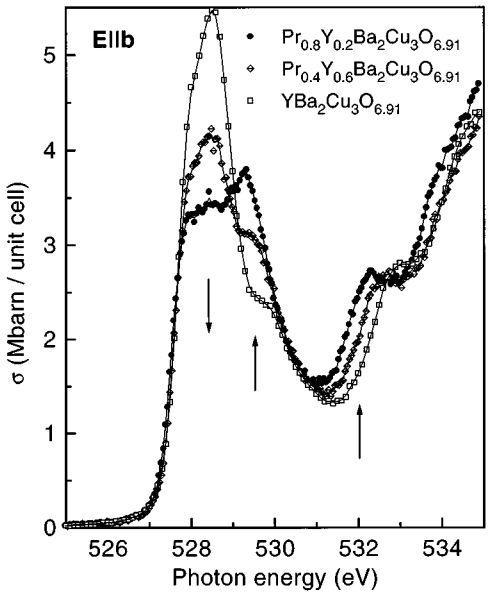

FIG. 4. O 1*s* absorption spectra of $Pr_{0.8}Y_{0.2}Ba_2Cu_3O_{6.91}$, $Pr_{0.4}Y_{0.6}Ba_2Cu_3O_{6.91}$, and $YBa_2Cu_3O_{6.91}$ for $\mathbf{E}\|b$. For $\mathbf{E}\|b$ an analogous trend is observed as for the $\mathbf{E}\|a$ spectra.

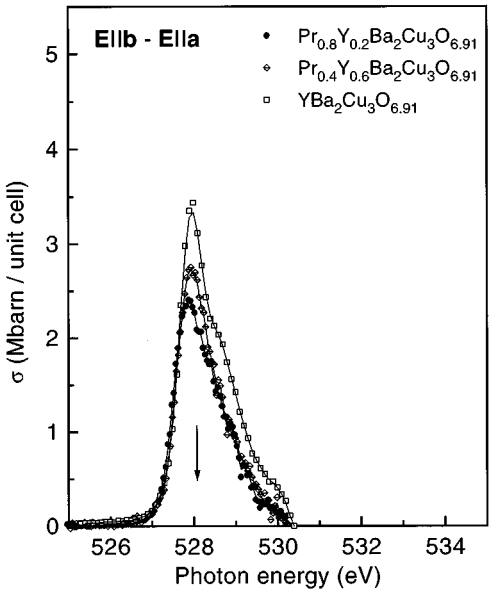

FIG. 5. Difference spectra $\mathbf{E}\|b-\mathbf{E}\|a$ for $Pr_{0.8}Y_{0.2}Ba_2Cu_3O_{6.91}$, $Pr_{0.4}Y_{0.6}Ba_2Cu_3O_{6.91}$, and $YBa_2Cu_3O_{6.91}$. Assuming only holes in σ orbitals, the contribution of the O(1) chain oxygen is derived from the enhanced spectral weight of $\mathbf{E}\|b$ compared to $\mathbf{E}\|a$. A reduction of this difference spectrum with increasing Pr concentration is evident.

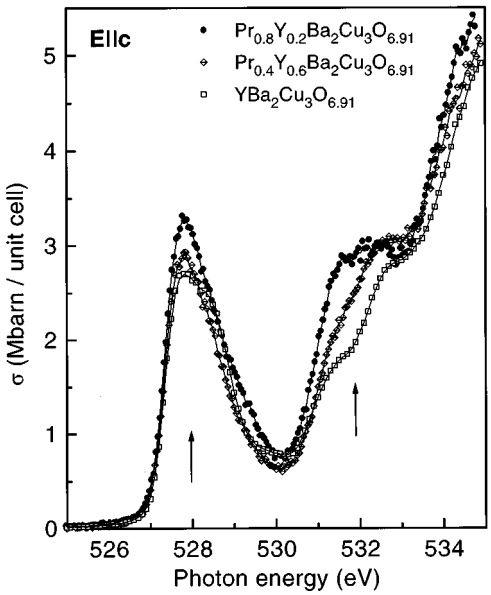

FIG. 6. $\mathbf{E}\|c$ spectra of $Pr_xY_{1-x}Ba_2Cu_3O_{6.91}$ ($x=0.8$, 0.4, 0.0). For $YBa_2Cu_3O_{6.91}$ the complete peak at 528 eV is ascribed to the apical oxgen atoms while for $Pr_{0.8}Y_{0.2}Ba_2Cu_3O_{6.91}$ the peak also contains contributions from the FR state.

butions to the pre-edge are caused by unoccupied O(2) $2p_x$ orbitals only while $\mathbf{E}\|b$ contributions should result from O(3) $2p_y$ orbitals in the CuO_2 planes and, additionally, from O(1) $2p_y$ orbitals in the CuO_3 chains. Since structural asymmetry between the Cu(2)-O(2) and the Cu(2)-O(3) bond lengths is small (1.4% for $Pr_{0.8}Y_{0.2}Ba_2Cu_3O_{6.91}$ and 1.7% for $YBa_2Cu_3O_{6.91}$; see Table I), the symmetry of the Cu(2) $3d_{x^2-y^2}$–O(2,3) $2p_{x,y}$ hybrids in the CuO_2 planes is only slightly distorted. Thus, from the point of view of the CuO_2 planes' electronic structure, equivalence of the a and b directions of the planes is expected to be a good approximation. In this approximation, the difference between the $\mathbf{E}\|b$ and the $\mathbf{E}\|a$ spectra can be ascribed to the contributions of the O(1) $2p_y$ orbitals in the CuO_3 chains. The contributions $\mathbf{E}\|b-\mathbf{E}\|a$ for the three samples are plotted in Fig. 5. A gradual decrease of the spectral intensity with increasing Pr concentration is observed. Starting at about 530.4 eV, the subtraction $\mathbf{E}\|b-\mathbf{E}\|a$ leads to negative values, regardless of the Pr concentration. This is due to the fact that the peak observed at 530.7 eV in the $\mathbf{E}\|a$ spectrum is absent for polarization $\mathbf{E}\|b$. Since the electronic structure of the planes is assumed to be equivalent along the a and b directions, the peak at 530.7 eV for $\mathbf{E}\|a$ may be interpreted as a hybridization between a linear combination $\beta_1|p_x\rangle+\beta_2|p_z\rangle$ of O(1) $2p$ orbitals with Ba states.

For $\mathbf{E}\|c$, only O(4) $2p_z$ orbitals contribute if holes in π-bonded O orbitals are neglected. The assumption that σ-bonded O orbitals are playing the leads is supported by the threshold energies of the pre-edges. Consistent with electron energy loss spectroscopy (EELS) data,[31,54] the O 1s threshold energy of $YBa_2Cu_3O_{6.91}$ is at 528.0 eV for $\mathbf{E}\|a$ and at 527.3 eV for $\mathbf{E}\|c$. Most band structure calculations predict that the O 1s level of the O(4) site has the lowest binding energy[55–57] and that, therefore, the threshold for $\mathbf{E}\|c$ should occur at the lowest photon energy. The $\mathbf{E}\|c$ absorption edges are depicted in Fig. 6. The spectra consist in this energy range of two main features: a peak at 528 eV and a broad shoulder extending from 531.5 eV to 533 eV. Both features show an increase of intensity with increasing Pr concentration. While the peak at 528 eV seems to be only slightly affected, a much stronger increase of spectral weight is observed for the broad shoulder. The peak at 528 eV has a constant width [full width at half maximum (FWHM)] of $\Delta E\approx 1.7$ eV for all Pr concentrations, which is broader by about 0.5 eV than the ZR states of the planes (Fig. 3). In previous work[21,58] the peak of $YBa_2Cu_3O_{6.91}$ was wholly ascribed to unoccupied states related to the O(4) apical oxygen atoms.

In Fig. 7, the $\mathbf{E}\|a$ spectra for the oxygen-deficient $Pr_xY_{1-x}Ba_2Cu_3O_{7-y}$ ($x=$ 0.8, 0.0) samples are plotted. For the oxygen-depleted $YBa_2Cu_3O_{7-y}$ crystal a small shoulder at 528.5 eV is observed. This shoulder is a consequence of a slight hole doping due to an enhanced oxygen content. In the case of the oxygen-deficient $Pr_{0.8}Y_{0.2}Ba_2Cu_3O_{7-y}$ sample such a shoulder is not observed. Employing optical reflectivity measurements, we estimated the oxygen content of $YBa_2Cu_3O_{7-y}$ and $Pr_{0.8}Y_{0.2}Ba_2Cu_3O_{7-y}$ to be 6.15 and 6.05, respectively,[43] as mentioned above. The NEXAFS data are corrected for self-absorption and saturation effects and normalized to the cross section of the actual oxygen content. However, our further discussion will not be affected by such a slight difference in the oxygen content of the crystals. Above 535 eV (not shown) the spectra of both samples are identical. Ignoring the small shoulder at 528.5 eV, $YBa_2Cu_3O_{6.15}$ exhibits its first peak at 530.0 eV. Since $YBa_2Cu_3O_{6.15}$ is an insulator and this peak belongs to the first unoccupied states above the Fermi level, this feature is ascribed to the oxygen states hybridized with the upper Hubbard band (UHB). For the $Pr_{0.8}Y_{0.2}Ba_2Cu_3O_{6.05}$ sample, the threshold energy of the

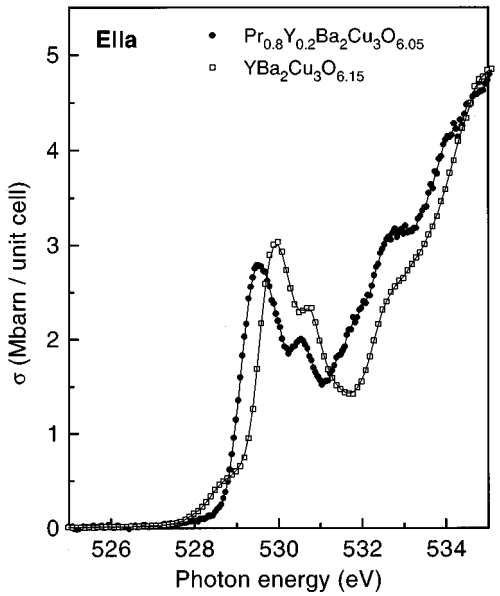

FIG. 7. O 1*s* absorption spectra of the O atoms in the plane for oxygen-deficient $Pr_{0.8}Y_{0.2}Ba_2Cu_3O_{6.05}$ and $YBa_2Cu_3O_{6.15}$. In both cases a distinct UHB is observed. The onset of the UHB of $Pr_{0.8}Y_{0.2}Ba_2Cu_3O_{6.05}$ is downshifted by $\approx$ 0.35 eV.

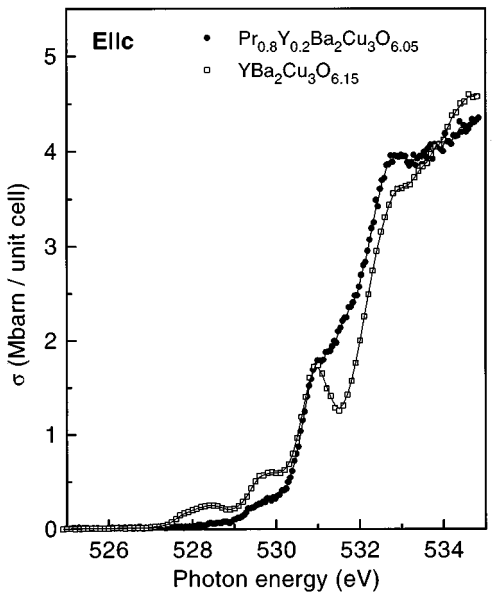

FIG. 8. O 1*s* absorption spectra of $Pr_{0.8}Y_{0.2}Ba_2Cu_3O_{6.05}$ and $YBa_2Cu_3O_{6.15}$ for polarization parallel to the *c* direction. For both samples an UHB is absent since the UHB has predominantly planar character.

UHB is shifted down by about 0.35 eV. This result is supported by optical measurements of oxygen-depleted samples which indicate a reduction of the charge transfer gap from $\Delta_{CT} \approx 1.7$ eV to 1.4 eV when the Pr concentration x is raised from 0.0 to 1.0.[32] The 0.35 eV downshift of the UHB, observed not only in the spectra of the oxygen-deficient but also in that of oxygen-rich samples (Fig. 10 and Fig. 3, respectively), confirms the view mentioned above that the O 1*s* core level together with E_F is shifted to higher energies with increasing x. The UHB downward shift can be explained by changes in the Madelung potentials which are caused by the much larger distance between adjacent CuO_2 planes in the case of $Pr_{0.8}Y_{0.2}Ba_2Cu_3O_{6.05}$ (Table I). In contrast to this large increase of the distance between neighboring planes, the in-plane Cu(2)-O(2) and Cu(2)-O(3) bond lengths are only slightly enlarged and, therefore, no significant intensity changes are observed between the UHB of $YBa_2Cu_3O_{6.15}$ and $Pr_{0.8}Y_{0.2}Ba_2Cu_3O_{6.05}$. As has been the case for the oxygen-rich crystals discussed above, for the oxygen-depleted crystals again additional spectral weight occurs between 531.5 eV and 533.0 eV for the Pr-doped sample.

Figure 8 shows the $\mathbf{E}\|c$ spectra of the oxygen-deficient samples. Since the UHB has predominantly planar character, these states vanish for $\mathbf{E}\|c$. The small peak at 528.5 eV for the $YBa_2Cu_3O_{6.15}$ sample is due to the slightly higher oxygen content, as was discussed above. From preliminary results from $PrBa_2Cu_3O_{6.1}$ (not shown), we conclude that the feature at 529.7 eV is most likely due to hybridization between oxygen and yttrium atoms. In earlier work we assigned the peak at 531.0 eV in the $YBa_2Cu_3O_{6.15}$ spectrum to transitions into the O(4)-Cu(1)-O(4) dumbbell of oxygen-depleted samples and regarded the intensity of this peak as a measure of vacant O(1) sites.[58] Studying our spectra, it becomes clear that for the Pr-doped sample no distinct peak is observed around 531.0 eV, but instead a broad shoulder. This may be due to contributions from higher-energy hybridizations by which this peak is drowned out. In the energy range between 531.5 eV and 533.0 eV the dip which is observed for $YBa_2Cu_3O_{6.15}$ is filled up with spectral weight for the Pr-doped sample. This additional intensity for $Pr_{0.8}Y_{0.2}Ba_2Cu_3O_{6.05}$ in the energy range between 531.5 eV and 533 eV is isotropic. It appears both for oxygen-deficient and oxygen-rich samples and grows with increasing Pr concentration. Since these unoccupied isotropic states are located 4–6 eV above the Fermi level, it can be ruled out that they are responsible for the suppression of superconductivity in the $Pr_xY_{1-x}Ba_2Cu_3O_{7-y}$ system. In previous NEXAFS measurements these isotropic states 4–6 eV above E_F were ascribed to Pr $4f_{z(x^2-y^2)}$–O $2p_\pi$ hybrids.[59]

A more thorough discussion of the features described in this section along with their implications for the electronic structure and the hole distribution on the structural units in $Pr_xY_{1-x}Ba_2Cu_3O_{7-y}$ will be given in the following section. We will also examine to what degree the various existing models, mentioned in the first section, agree with our data.

IV. DISCUSSION

A. Electronic structure of $Pr_xY_{1-x}Ba_2Cu_3O_{7-y}$ and charge distribution between the structural units

Considering a charge-transfer model for the Cu(2)-O(2,3) planes of $YBa_2Cu_3O_{6.0}$, the spectral weight for electron addition experiments (e.g., NEXAFS) contains an unoccupied UHB with Cu 3*d* character above the Fermi level, and the spectral weight for electron removal experiments (e.g., photoemission) shows a valence band with O 2*p* character below the Fermi level. In this picture, with increasing oxygen doping E_F is shifted below the top of the ligand band and holes will be created exclusively on oxygen sites. This

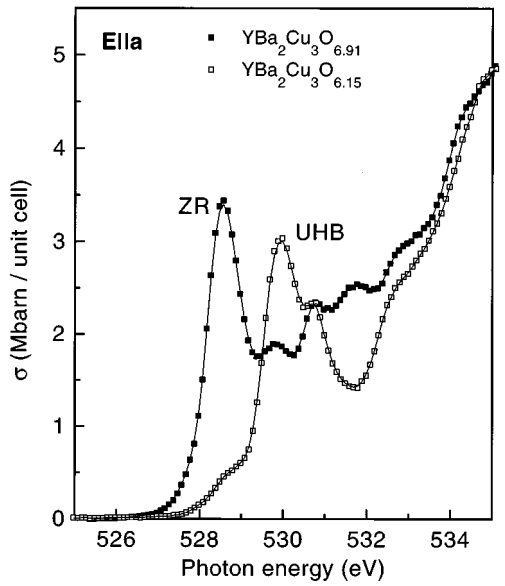

FIG. 9. Comparison of the O 1*s* absorption spectra of $YBa_2Cu_3O_{6.91}$ and its oxygen-deficient counterpart $YBa_2Cu_3O_{6.15}$ for polarization $\mathbf{E}\|a$. The ZR state is about 1.4 eV below the UHB.

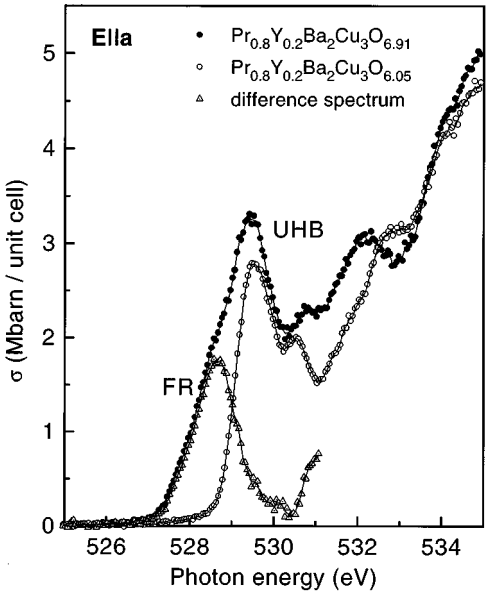

FIG. 10. Comparison of the O 1*s* absorption spectra of $Pr_{0.8}Y_{0.2}Ba_2Cu_3O_{6.91}$ and $Pr_{0.8}Y_{0.2}Ba_2Cu_3O_{6.05}$ for polarization $\mathbf{E}\|a$. For both oxygen concentrations the peak position of the UHB is at the same energy. Therefore, the spectrum of $Pr_{0.8}Y_{0.2}Ba_2Cu_3O_{6.91}$ is assumed to consist of an UHB plus additional spectral weight on the low-energy side of the UHB.

picture changes if hybridization between O and Cu atoms is included. With increasing hybridization, i.e., with larger hopping integral t_{pd} between Cu $3d_{x^2-y^2}$ and O $2p_{x,y}$ orbitals, Cu 3*d* states are mixed into the valence band and O 2*p* states are admixed to the UHB. Hybridization then causes correlation effects on copper sites to be important for the valence band and the ZR state as well (see also Ref. 36). In effect, it leads to a transfer of spectral weight from the UHB to the ZR state upon oxygen doping.[60,61] This is demonstrated in Fig. 9 where the $\mathbf{E}\|a$ spectra of oxygen-depleted ($y\approx 0.9$) and almost fully oxygenated ($y\approx 0.1$) $YBa_2Cu_3O_{7-y}$ samples are depicted: At higher O content the UHB is reduced while the ZR band is strongly increased. The ZR state is located at 1.4 eV below the UHB. If we now compare the $\mathbf{E}\|a$ spectra of oxygen-deficient and oxygen-rich $Pr_{0.8}Y_{0.2}Ba_2Cu_3O_{7-y}$ (Fig. 10), we note that both show a strong UHB peak at 529.5 eV. In the $Pr_{0.8}Y_{0.2}Ba_2Cu_3O_{6.91}$ spectrum, however, much more spectral weight on the low-energy side of the UHB is observed, as depicted by the difference spectrum in Fig. 10. From Fig. 3 it is evident that these additional states are located in the energy range between E_F (known from the onset of the $YBa_2Cu_3O_{6.91}$ spectrum) and the peak position of the UHB of $Pr_{0.8}Y_{0.2}Ba_2Cu_3O_{6.05}$. Therefore, these additional states in $Pr_{0.8}Y_{0.2}Ba_2Cu_3O_{6.91}$ are located in the same energy range as the ZR state in $YBa_2Cu_3O_{6.91}$. For oxygen-rich samples, the additional spectral weight in the energy range between E_F and the UHB together with the UHB itself rises at the expense of the ZR state (Fig. 3), as the Pr content increases. Considering Fig. 11, we emphasize that if the holes were residing in the ZR state, transitions from the O 1*s* core level into the UHB would exhibit little spectral weight due to the transfer of spectral weight from the UHB to the ZR state.[21,58,60,61] In contrast to this, the spectral weight of the UHB should be observed with the same strength as for oxygen-depleted $YBa_2Cu_3O_{6.15}$ or $Pr_{0.8}Y_{0.2}Ba_2Cu_3O_{6.05}$ if the holes are moved from the ZR state into states which have no hybridization with Cu atoms and, therefore, are unaffected by correlation effects on Cu sites. Since for $Pr_{0.8}Y_{0.2}Ba_2Cu_3O_{6.91}$ an UHB is observed which is as intense as for $YBa_2Cu_3O_{6.15}$ or $Pr_{0.8}Y_{0.2}Ba_2Cu_3O_{6.05}$, we can draw the conclusion that with increasing Pr concentration holes are pushed out of the ZR state and moved into the energetically favored additional states on the low-energy side of the UHB (Fig. 10) which

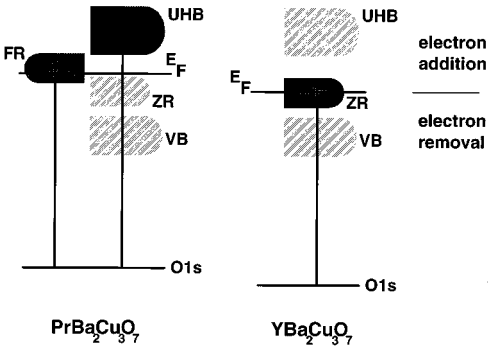

FIG. 11. A sketch of the expected electronic structure if the holes reside on the ZR state (like in $YBa_2Cu_3O_7$) or if they reside on the FR state (such as proposed for $PrBa_2Cu_3O_7$). With increasing Pr concentration x, E_F moves towards the top of the ZR state and, finally, for sufficiently high x E_F lies above the upper edge of the ZR state. If the holes reside on the ZR state ($YBa_2Cu_3O_7$), transitions from the O 1*s* core level into the UHB play only a minor role due to the Cu correlation-mediated transfer of spectral weight to lower energies. If, on the other hand, the holes reside on the FR state ($PrBa_2Cu_3O_7$), this Cu correlation effect is absent and, thus, transitions from the core level into both the FR state and the UHB are observed.

TABLE II. The hole distribution between the structural units of $Pr_{1-x}Y_xBa_2Cu_3O_{6.91}$. The contributions n_a, n_{chain}, and n_c are obtained from the $\mathbf{E}\|a$, $\mathbf{E}\|b-\mathbf{E}\|a$, and $\mathbf{E}\|c$ NEXAFS spectra, respectively, and n_{tot} is the total amount of holes observed on all oxygen sites. For $x=0.0$ and 0.4 the contribution $2n_a$ is ascribed to the ZR state. For $x=0.8$ this contribution is ascribed to the FR state plus a small amount of holes left in the ZR state due to the 20% Y in the compound.

	$x=0.0$	$x=0.4$	$x=0.8$
$2n_a$	0.40	0.29	0.25
n_{chain}	0.24	0.18	0.17
n_c	0.27	0.27	0.31
n_{tot}	0.91	0.74	0.73

have no copper character. Thus, O $2p_\sigma$ states[34] can be ruled out. The fact that the holes are removed from the ZR state is reflected on the one hand by the strong reduction of the ZR state and on the other hand by the strong increase of the UHB as shown in Figs. 3 and 10. Therefore, we regard the feature extending from 527.0 eV to 530.2 eV for $Pr_{0.8}Y_{0.2}Ba_2Cu_3O_{6.91}$ (Fig. 10) as a combination of an UHB like that of $Pr_{0.8}Y_{0.2}Ba_2Cu_3O_{6.05}$ plus additional states on the low-energy side of the UHB. On the high-energy side additional spectral weight is not only observed for $Pr_{0.8}Y_{0.2}Ba_2Cu_3O_{6.91}$ but also for $YBa_2Cu_3O_{6.91}$ compared to their oxygen-depleted counterparts (Figs. 9 and 10) and is, therefore, attributed to a generally higher degree of hybridization in this energy range, independent of the Pr concentration.

Unfortunately, the amount of spectral weight transferred to lower energies upon doping has not been calculated for this system up to now. To nevertheless obtain an estimate of the number of holes residing on the various structural units, we are forced to consider the additional spectral weight on the low-energy side of the UHB to be proportional to the Pr concentration x and to the oxygen content $7-y$, despite the existence of the gradual transfer of spectral weight mentioned above. For $YBa_2Cu_3O_7$, the total number of holes per unit cell residing on the O sites was assumed to be 1. The total integrated cross section of the seven O sites in $YBa_2Cu_3O_{6.91}$ then corresponds to 17.8 Mb eV/unit cell. Using this scaling factor, the site-specific and Pr-concentration-dependent hole numbers were derived from the integrated cross sections of the first absorption peak in the O 1*s* spectra of the O(1) atom (Fig. 5), of the four O(2,3) atoms (Fig. 3), and of the two O(4) atoms (Fig. 6). We point out that only about 80% of the holes which reside in $YBa_2Cu_3O_{6.91}$ on oxygen sites are found for $Pr_{0.8}Y_{0.2}Ba_2Cu_3O_{6.91}$ and also for $Pr_{0.4}Y_{0.6}Ba_2Cu_3O_{6.91}$. For all Pr concentrations measured, the holes observed for different light polarizations are listed in Table II. A total of about 0.4 holes is observed for $YBa_2Cu_3O_{6.91}$ on both the O(2) and O(3) sites of the planes ($2\mathbf{E}\|a$). When the Pr concentration is increased, the number of holes in both planes is gradually reduced. In other words, the Fermi level is moved up towards the top of the ZR band. For $Pr_{0.4}Y_{0.6}Ba_2Cu_3O_{6.91}$, still about 0.15 holes per plane are residing on planar oxygen orbitals forming the ZR band. Therefore, the sample still exhibits metallicity and superconductivity. This is consistent with previous NEXAFS investigations on a series of $YBa_2Cu_3O_{7-y}$ single crystals with different O stoichiometries where it was shown that similar amounts of O-doped holes per CuO_2 plane lead to similar T_c's.[58] For further Pr doping, the holes in the ZR band are increasingly filled up, and at the same time the amount of holes residing on the additional states which are competitive in energy with the ZR state is growing. Finally, for $Pr_{0.8}Y_{0.2}Ba_2Cu_3O_{6.91}$, no doped holes reside on the ZR state, i.e., on O(2,3) $2p_\sigma$ orbitals,[34] but rather are all on these additional states. Unfortunately, it cannot be distinguished by our experiments if there exists a gap between the ZR and FR bands or if these two bands exhibit an overlap (see sketch of electronic structure in Fig. 11). In the former case, the insulating behavior of the sample would be explainable by the existence of the gap. In the latter, E_F is located above the upper edge of the ZR band but also above the bottom of the FR band, implying that the suppression of metallicity must be related to an extrinsic origin.

The contribution of the O(1) site, obtained by the difference spectra $\mathbf{E}\|b-\mathbf{E}\|a$, is also gradually reduced on raising the Pr content. For $Pr_{0.4}Y_{0.6}Ba_2Cu_3O_{6.91}$ this contribution has already fallen from 0.24 to 0.18 holes per O(1) site while the slight decrease upon further doping (see Table II) can hardly be regarded as significant. Hence, the contribution from the O(1) atoms seems to be already strongly altered at low doping concentrations due to the presence of Pr atoms and shows saturation at larger Pr content. The number of holes residing on the apical O(4) site is not changed at all by increasing the Pr concentration to 0.4 but the number of holes observed for $\mathbf{E}\|c$ is slightly enhanced from 0.27 to 0.31 holes if the Pr-doping concentration is increased to 0.8. Thus, in contrast to the O(1) site, the $\mathbf{E}\|c$ hole count is slightly increased and is mostly affected at higher Pr concentrations. This implies that the total amount of holes residing on the CuO_3 chains is slightly reduced. This small decrease of holes on the chain sites is in accordance with recent optical investigations[62] where a reduction by about 14% of the amount of holes residing on the CuO_3 chains was reported. Furthermore, NMR and nuclear quadrupole resonance (NQR) data[15,18,63,64] have shown that for a fixed oxygen concentration the electric field gradients at the Cu(1) and at the apical O(4) site remain almost unchanged, regardless of the *R* substituent in $RBa_2Cu_3O_{7-y}$. Therefore, a substantial charge transfer in connection with the apical O(4) site can be excluded.

To estimate the number of holes residing on the additional planar states on the low-energy side of the UHB (Fig. 10), we have subtracted the UHB of the $\mathbf{E}\|a$ spectrum of the oxygen-depleted $Pr_{0.8}Y_{0.2}Ba_2Cu_3O_{6.05}$ sample from the $\mathbf{E}\|a$ spectrum of the oxygen-rich $Pr_{0.8}Y_{0.2}Ba_2Cu_3O_{6.91}$ crystal. The resulting difference spectrum is depicted in Fig. 10. The integrated spectral weight of the difference spectrum corresponds to 0.25 holes per unit cell. Since we observe for $YBa_2Cu_3O_{6.91}$ a total of 0.91 holes and in the case of $Pr_{0.8}Y_{0.2}Ba_2Cu_3O_{6.91}$ just 0.73 holes, we assume that the missing 0.18 holes reside on Pr.[48] Thus, we can draw the following conclusions: With increasing Pr concentration a total of about 0.2 holes is transferred away from the ZR state and the O(1) site, and is probably moved to Pr. Upon further increasing the Pr concentration 0.25 holes are moved from

the ZR state into the energetically favored states on the low-energy side of the UHB. These additional states are not hybridized with Cu. The apical O(4) site remains essentially unaffected by Pr doping.

B. Comparison with current models

Based on these quantifications we can finally examine the various models mentioned in Sec. I. As we already pointed out in Sec. III, the model of Ref. 40 fails to describe our results since disorder effects at the Ba site are inconsistent with our neutron diffraction and EDX results.

It is also evident from the NEXAFS data that a gradual redistribution of the doped holes from the CuO_2 planes to the CuO_3 chains as proposed in Ref. 39 can be ruled out, too. Instead of a hole *increase* on the oxygen sites of the CuO_3 chain, as expected in this model, we do in fact observe a *decrease* by 14% of the total hole count on the chain. Further support for this comes from optical experiments[54] also reporting a decrease of 14%.

The rest of this section will be devoted to discussing aspects of a Pr $4f_{z(x^2-y^2)}$–O $2p_\pi$ hybridization[33,37] and their consequences for the electronic structure observed in NEXAFS. According to Fehrenbacher and Rice, the substitution of Y by Pr causes the initially delocalized holes to be moved from in-plane O(2,3) $2p_\sigma$ orbitals to the O(2,3) $2p_\pi$ orbitals hybridized with the central Pr.[34] The UHB band will then be visible since in this case there is no transfer of spectral weight from the UHB to the ZR state (see Fig. 11). As already pointed out above this lack of transfer of spectral weight is indeed observed in our spectra. Therefore, we assume that the feature at 529.5 eV in the $\mathbf{E}\|a$ spectrum of $Pr_{0.8}Y_{0.2}Ba_2Cu_3O_{6.91}$ is composed of an UHB like that of $Pr_{0.8}Y_{0.2}Ba_2Cu_3O_{6.05}$ plus possible FR states (Fig. 10). We will now examine if the above-mentioned additional low-energy states are in fact consistent with further characteristics of FR states. In the FR model it was assumed that the O(2,3) $2p_\pi$ orbitals point towards the central Pr ion, which means a rotation of the O $2p_\pi$ orbitals of about 45°.[34] Therefore, an *isotropic*[34] contribution from in-plane transitions and from transitions perpendicular to the CuO_2 planes should be observed if the FR states can be identified with the additional states observed in the spectra. To obtain a numerical estimate of these states, we have to take into consideration, that only O $1s$–O $2p_z$ transitions are allowed for $\mathbf{E}\|c$ while, for $\mathbf{E}\perp c$, O $1s$–O $2p_x$ and O $1s$–O $2p_y$ transitions are possible. This implies that in the former case all orbitals are involved in the absorption process but in the latter half the orbitals are oriented perpendicular to the polarization vector of the synchrotron radiation. Hence, the difference spectrum $(Pr_{0.8}Y_{0.2}Ba_2Cu_3O_{6.91}-Pr_{0.8}Y_{0.2}Ba_2Cu_3O_{6.05})$ for polarization $\mathbf{E}\|a$ has to be scaled by a factor of 2 in order to take all planar contributions into account. The scaled difference spectrum is shown in Fig. 12 together with the $\mathbf{E}\|c$ spectrum of $Pr_{0.8}Y_{0.2}Ba_2Cu_3O_{6.91}$. The common area below both curves can be regarded as an upper limit for isotropic Fehrenbacher-Rice states.[33,34] The integrated area common to both curves corresponds to 0.21 holes. This accounts for only half the states since the orbitals are assumed to be rotated by 45°. Therefore, a total of 0.42 holes could reside on the possible FR state. The peak of the $\mathbf{E}\|c$ absorption spectrum amounting in total to 0.31 holes would then be composed of a FR component and a component due to the apical oxygen which implies that 0.21 holes would correspond to the FR state and only 0.10 holes would be left on the apical O(4) site. Since we can exclude such a small number of holes on the apical O(4) site if optical[32,62] and NMR data[15,18,63,64] are taken into account, this places an extra and quite tough constraint on the FR state, which cannot be reconciled with the original FR approach (45° rotation of the O $2p_\pi$ orbitals).

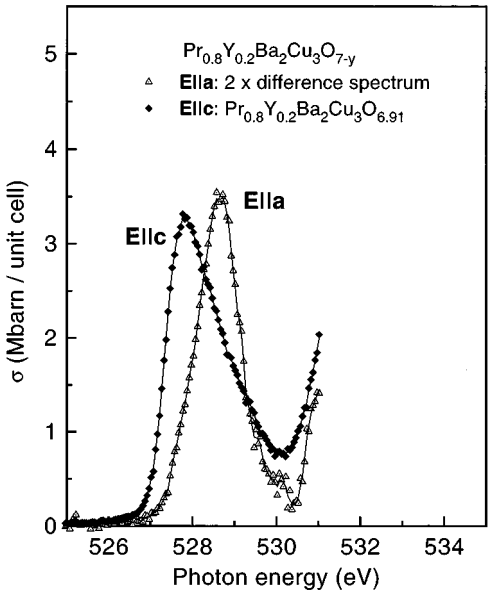

FIG. 12. Comparison of the planar difference spectrum $2(Pr_{0.8}Y_{0.2}Ba_2Cu_3O_{6.91}-Pr_{0.8}Y_{0.2}Ba_2Cu_3O_{6.05})$ and the $\mathbf{E}\|c$ spectrum of $Pr_{0.8}Y_{0.2}Ba_2Cu_3O_{6.91}$. The area enclosed by both curves constitutes an upper limit for *isotropic* FR states.

Combining our results with optical data,[62] it is evident that the reduction of holes residing on O sites of the chain takes place predominantly on the O(1) site since the reduction by about 14% of the chain holes is already fulfilled by the O(1) hole decrease as can be inferred from Table II. This conclusion is corroborated by NMR data[63,64] where no changes for the O(4) and Cu(1) sites were detected. Thus, it can be concluded that the number of holes on the apical O(4) site remains unaffected by Pr substitution while the decrease of O(1) holes is responsible for the 14% reduction of the chain holes. Even with this reduction, there are still 0.44 holes located on the chain unit of $Pr_{0.8}Y_{0.2}Ba_2Cu_3O_{6.91}$. This refutes the approach of Wang *et al.*,[38] according to which *no* holes are left in the CuO_3 chains.

In contrast to the *isotropic* FR state[34] suggested in the FR model,[33] Liechtenstein and Mazin[37] (LM) proposed that the FR state which grabs the holes has exclusively *planar* character. They have calculated the Pr-concentration-dependent number of holes in this planar FR state. For $Pr_{0.8}Y_{0.2}Ba_2Cu_3O_7$ they find 0.25 holes, exactly the value we observe in the additional planar states on the low-energy side of the UHB (see Fig. 10 and Table II). However, they consider a dispersive and conducting $pd\pi$ band with a hopping integral $t_{pf}=0.75$ eV between the FR state and Pr $4f$ orbitals. In order to obtain a narrow band and, therefore, insulating behavior, they have to resort to strong scattering

effects due to more than 6% Ba on the Pr site. Although the number of holes in *planar* FR states is consistent with the NEXAFS data of $Pr_{0.8}Y_{0.2}Ba_2Cu_3O_{6.91}$, this scattering due to Ba on the Pr site as invoked by Liechtenstein and Mazin[37] is inconsistent with the findings of the neutron diffraction measurements, as mentioned above. By and large, it may be said that the LM approach would, in principle, agree with our NEXAFS data if the FR band exhibited greater p_z character above E_F than expected from Fig. 1 in Ref. 37.

Based on the idea that the rotation angle may be situated somewhere between the two suggested extremes of 0° and 45°, we propose a very simple and straightforward extension of the original FR calculations. For this extension, a simple dependence on the rotation angle is introduced while all other results of Ref. 33 are retained unchanged. According to this, the peak at 528.7 eV for $\mathbf{E}\|a$ in Fig. 12 consists of holes in the FR state plus holes which remain in the ZR state due to the Y fraction in the material, while the $\mathbf{E}\|c$ feature at 527.8 eV is composed of holes in the FR state plus holes on the apical oxygen. By changing the rotation angle of the O(2,3) $2p_\pi$ orbitals the contribution of the FR state to the $\mathbf{E}\|c$ spectrum can then be varied. We assume that for rotation angles $\neq 45°$ a FR state is still possible. In the original FR model, the FR state with a rotation angle of 45° is stabilized if the hopping matrix element between O $2p$ and Pr $4f$ states, t_{pf}, is in the range 0.4–0.5 eV. This range of values for t_{pf} appears to be a sensible requirement for the stability of a FR state at a rotation angle $\gamma \neq 45°$ as well. In other words, we consider 0.4 eV$\leqslant t_{pf} \leqslant$0.5 eV as the criterion for a stable FR state for any given rotation angle $\neq 45°$, regardless of the maximum value that t_{pf} reaches around 45°.

Moreover, we assume that all of the missing 0.18 holes in $Pr_{0.8}Y_{0.2}Ba_2Cu_3O_{6.91}$ are transferred to Pr. Hence, consistent with the Fehrenbacher-Rice model,[33] we ascribe a valence of +3.18 to Pr. For our simple extension of the FR model up to $n_{ZR} \leqslant 0.2$ holes were allowed in the ZR state since 20% Y is left in the compound. The contributions determined from our NEXAFS data for $\mathbf{E}\|a$, n_a, $\mathbf{E}\|b$, n_b, and $\mathbf{E}\|c$, n_c, were, of course, incorporated into our extension. The number of apical O(4) holes depending on the rotation angle of the O(2,3) $2p_\pi$ orbitals can then be obtained utilizing the following relations:

$$
\begin{aligned}
n_{\mathrm{Pr}} &= n_F(2-n_f),\\
n_{\mathrm{FR}} &= n_F(n_f-1),\\
2n_a &= n_{\mathrm{FR}}\cos^2\gamma + n_{\mathrm{ZR}},\\
n_c &= n_{\mathrm{FR}}\sin^2\gamma + n_{\mathrm{apex}},\\
n_{\mathrm{Pr}} + n_{\mathrm{FR}} + n_{\mathrm{ZR}} + n_{\mathrm{apex}} + n_{\mathrm{chain}} &= 0.91,
\end{aligned}
\tag{3}
$$

where n_{Pr} denotes the number of holes transferred to Pr, n_{FR} the number of holes situated on the O $2p_\pi$ orbitals, n_F the density of Pr^{IV} ions, n_f the number of Pr $4f$ electrons, γ the rotation angle of the O $2p_\pi$ orbitals, n_{ZR} the number of holes situated on the O $2p_\sigma$ orbitals, n_{apex} the number of holes on the O(4) site, and n_{chain} the number of holes on the O(1) site. The results are depicted in Fig. 13. Using the relationship between t_{pf} and n_f given in Table I of Ref. 33, the FR state is stabilized for the solid curves ($1.58 < n_f < 1.66$). For the dotted curves below the stable range the $4f$ occupation n_f is too large (>1.66) and the corresponding t_{pf} too small to stabilize the FR state. In this case the superconducting solution, i.e., the ZR state, is energetically favored. For the dotted curves above the stable range ($n_f < 1.58$) n_F becomes too small ($\leqslant 0.4$), and at the same time the hopping integral t_{pf} required (>0.5 eV) becomes even harder to reconcile with the insulating behavior observed. The restriction ''unchanged apical hole concentration'' and the suggestion of a 45° rotation of the O(2,3) $2p_\pi$ orbitals are represented by dashed lines in the figure. It is obvious from Fig. 13 that one can have a stable FR state and an unchanged apical hole concentration at the same time if the O(2,3) $2p_\pi$ orbitals are rotated out of the plane by just about 20°–25°.

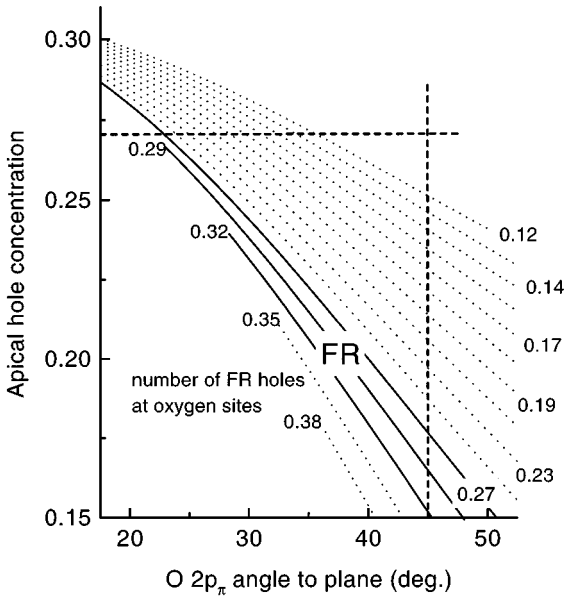

FIG. 13. Test of the Fehrenbacher-Rice model. The apical hole concentration is depicted as a function of the rotation angle of the O(2,3) $2p_\pi$ orbitals, as calculated from Eq. (3) (in the text). NEXAFS results of this work are incorporated (see text).

This result differs from the proposed extremes of 45° rotation in the FR model and of 0° rotation in the LM approach. However, the NEXAFS data are consistent with a Pr $4f_{z(x^2-y^2)}$–O $2p_\pi$ hybridization and indicate a rotation angle of the O $2p_\pi$ orbitals that is situated in the middle of the proposed ones.

V. CONCLUSIONS

In summary, we have conducted NEXAFS and neutron diffraction measurements on $Pr_{1-x}Y_xBa_2Cu_3O_{7-y}$ single crystals with different Pr and O concentrations. The main result of our investigations is that we can rule out models involving hole filling or charge transfer between the planes and the chains while our data are consistent with approaches based upon Pr $4f$–O(2,3) $2p_\pi$ hybridization. From our measurements the following picture for the electronic structure of $Pr_{1-x}Y_xBa_2Cu_3O_{6.91}$ arises: Due to Pr doping of $YBa_2Cu_3O_{6.91}$, at first about 0.2 holes are lost from the O

subsystem and presumably transferred from O(1) and O(2,3) sites to the Pr atom. On further doping the additional states on the low-energy side of the UHB are stabilized and about 0.3 holes are transferred from the energetically competing ZR state to these additional states. If the additional states are interpreted as FR states, they neither have the proposed rotation angle of 45° (FR model) nor do they show exclusively planar character (LM approach); rather, the O(2,3) $2p_\pi$ orbitals are rotated by an angle of about 20°–25°. Therefore, for $Pr_{0.8}Y_{0.2}Ba_2Cu_3O_{6.91}$ about $n_{\rm apex}+n_{\rm chain}\approx 0.5$ holes still reside on the oxygen chain sites, $n_{\rm Pr}\approx 0.2$ holes are presumably transferred to the Pr atom, and $n_{\rm FR}\approx 0.3$ holes are moved from the ZR state into the energetically favored FR states. Following the arguments of Fehrenbacher and Rice[33] and those of Liechtenstein and Mazin,[37] it is likely that an enhanced t_{pf} for Pr as compared to other rare earths or Y combined with favorable values of ϵ_f and U_f is responsible for the stability of the FR state. The discrepancy in the rotation angle of the p_π orbitals between our NEXAFS data and theory may be due to the fact that in the calculations of Ref. 33 possible effects of the copper potentials on the Pr $4f$–O(2,3) $2p_\pi$ hybridized state are neglected, and that in Ref. 37 correlation effects on the copper sites are disregarded.

ACKNOWLEDGMENTS

We are grateful to K. Widder and H. P. Geserich for performing the optical reflectivity measurements on oxygen-deficient $Pr_xY_{1-x}Ba_2Cu_3O_{7-y}$ and for stimulating discussions. We greatly appreciate fruitful discussions with R. Fehrenbacher and I. Mazin. We thank H. Winter, B. Seibel, E. Seibel, and S.-L. Drechsler for clarifying comments about theoretical aspects, B. Scheerer for his excellent technical support, and E. Sohmen and J.-H. Park for their experimental assistance. We are indebted to G. Meigs for his very generous help in sorting out technical difficulties. P. Adelmann provided valuable insight into the chemistry of impurities. The NSLS is part of Brookhaven National Laboratory, which is funded by the U.S. DOE. Part of this work was supported by the EU under Contract No. SCI CT91-0751 and the HCM network under Contract No. ERB CH RXCT 940438. V.C. was supported by the Office of Naval Research. M.S.G. is grateful for support from the HCM program of the EU.

*Present address: Materials Science Centre, University of Groningen, Nijenborgh 4, NL-9747 AG Groningen, The Netherlands.

[1] J. G. Bednorz and K. A. Müller, Z. Phys. B **64**, 189 (1986).

[2] M. K. Wu, I. R. Ashburn, C. J. Torng, P. H. Hor, R. L. Meng, L. Gao, Z. J. Huang, Y. Q. Wang, and C. W. Chu, Phys. Rev. Lett. **58**, 908 (1987).

[3] Z. Fisk, J. D. Thompson, E. Zirngiebl, J. L. Smith, and S.-W. Cheong, Solid State Commun. **62**, 743 (1987).

[4] P. H. Hor, R. L. Meng, Y. Q. Wang, L. Gao, Z. J. Huang, J. Bechtold, K. Forster, and C. W. Chu, Phys. Rev. Lett. **58**, 1891 (1987).

[5] M. B. Maple, Y. Dalichaouch, J. M. Ferreira, R. R. Hake, B. W. Lee, J. J. Neumeier, M. S. Torkachvili, K. N. Yang, H. Zhou, R. P. Guertin, and M. V. Kuric, Physica B **148**, 155 (1987), and references therein.

[6] Y. Dalichaouch, M. S. Torkachvili, E. A. Early, B. W. Lee, C. L. Seaman, K. N. Yang, H. Zhou, and M. B. Maple, Solid State Commun. **65**, 1001 (1988).

[7] B. Fisher, J. Genossar, L. Patlagan, and J. Ashkenazi, Phys. Rev. B **43**, 2821 (1991).

[8] A. Matsuda, K. Kinoshita, T. Ishii, H. Shibata, T. Watanabe, and T. Yamada, Phys. Rev. B **38**, 2910 (1988).

[9] A. P. Gonçalves, I. C. Santos, E. B. Lopes, R. T. Henriques, and M. Almeida, Phys. Rev. B **37**, 7476 (1988).

[10] Z. Quirui, Z. H. Zhenhui, Z. Han, X. Jiansheng, W. Shenxi, and F. Minghu, Physica C **162-164**, 963 (1989).

[11] L. Søderholm, K. Zhang, D. G. Hinks, M. A. Beno, J. D. Jorgensen, C. U. Segre, and I. K. Schuller, Nature **328**, 604 (1987).

[12] A. Kebede, C. S. Jee, J. Schwegler, J. E. Crow, T. Mihalisin, G. H. Myer, R. E. Salomon, P. Schlottmann, M. V. Kuric, S. H. Bloom, and R. P. Guertin, Phys. Rev. B **40**, 4453 (1989).

[13] J. L. Peng, P. Klavins, R. N. Shelton, H. B. Radousky, P. A. Hahn, and L. Bernardez, Phys. Rev. B **40**, 4517 (1989).

[14] J. J. Neumeier, Ph.D. thesis, University of California, San Diego, 1990.

[15] A. P. Reyes, D. E. MacLaughlin, M. Takigawa, P. C. Hammel, R. H. Heffner, J. D. Thompson, J. E. Crow, A. Kebede, T. Mihalisin, and J. Schwegler, Phys. Rev. B **42**, 2688 (1990); A. P. Reyes, D. E. MacLaughlin, M. Takigawa, P. C. Hammel, R. H. Heffner, J. D. Thompson, and J. E. Crow, *ibid.* **43**, 2989 (1991).

[16] D. W. Cooke, R. S. Kwok, R. L. Lichti, T. R. Adams, C. Boekema, W. K. Dawson, A. Kebede, J. Schwegler, J. E. Crow, and T. Mihalisin, Phys. Rev. B **41**, 4801 (1990); D. W. Cooke, M. S. Jahan, R. S. Kwok, R. L. Lichti, T. R. Adams, C. Boekema, W. K. Dawson, A. Kebede, J. Schwegler, J. E. Crow, and T. Mihalisin, Hyperfine Interact. **63**, 213 (1990).

[17] I. Felner, U. Yaron, I. Nowik, E. R. Bauminger, Y. Wolfus, E. R. Yacoby, G. Hilscher, and N. Pillmayr, Phys. Rev. B **40**, 6739 (1989).

[18] K. Nehrke, M. W. Pieper, and T. Wolf, Phys. Rev. B **53**, 1 (1996); K. Nehrke and M. W. Pieper, Phys. Rev. Lett. **76**, 1936 (1996).

[19] D. P. Norton, D. H. Lowndes, B. C. Sales, J. D. Budai, B. C. Chakoumakos, and H. R. Kerchner, Phys. Rev. Lett. **66**, 1537 (1991).

[20] N. Nücker, J. Fink, J. C. Fuggle, P. J. Durham, and W. M. Temmerman, Phys. Rev. B **37**, 5158 (1988).

[21] J. Fink, N. Nücker, E. Pellegrin, H. Romberg, M. Alexander, and M. Knupfer, J. Electron Spectrosc. Relat. Phenom. **66**, 395 (1994).

[22] J. J. Neumeier, T. Bjørnholm, M. B. Maple, J. J. Rhyne, and J. A. Gotaas, Physica C **166**, 191 (1990).

[23] M. Guillaume, P. Allenspach, J. Mesot, B. Roessli, U. Staub, P. Fisher, and A. Furrer, Z. Phys. B **90**, 13 (1993).

[24] M. E. López-Morales, D. Rios-Jara, J. Tagüeña, R. Escudero, S. La Placa, A. Bezinge, V. Y. Lee, E. M. Engler, and P. M. Grant, Phys. Rev. B **41**, 6655 (1990).

[25] L. Søderholm, C.-K. Loong, G. I. Goodman, and B. D. Dabrowski, Phys. Rev. B **43**, 7923 (1991).

[26] G. Hilscher, E. Holland-Moritz, T. Holubar, H.-D. Jostarndt, V. Nekvasil, G. Schaudy, U. Walter, and G. Fillion, Phys. Rev. B **49**, 535 (1994).

[27] G. Y. Guo and W. M. Temmerman, Phys. Rev. B **41**, 6372 (1990).

[28] J. S. Kang, J. W. Allen, Z.-X. Shen, W. P. Ellis, J. J. Yeh, B. W. Lee, M. B. Maple, W. E. Spicer, and I. Lindau, J. Less Common Met. **148**, 121 (1989).

[29] S. Horn, J. Cai, S. A. Shaheen, Y. Jeon, M. Croft, C. L. Chang, and M. L. den Boer, Phys. Rev. B **36**, 3895 (1987).

[30] U. Neukirch, C. T. Simmons, D. Sladeczek, C. Laubschat, O. Strebel, G. Kaindl, and D. D. Sarma, Europhys. Lett. **5**, 567 (1988).

[31] J. Fink, N. Nücker, H. Romberg, M. Alexander, M. B. Maple, J. J. Neumeier, and J. W. Allen, Phys. Rev. B **42**, 4823 (1990).

[32] K. Takenaka, Y. Imanaka, K. Tamasaku, T. Ito, and S. Uchida, Phys. Rev. B **46**, 5833 (1992).

[33] R. Fehrenbacher and T. M. Rice, Phys. Rev. Lett. **70**, 3471 (1993).

[34] We denote by ''O $2p_\pi$'' those orbitals on the O(2,3) sites that are perpendicular to the ones pointing towards the Cu(2) atoms (O $2p_\sigma$). In the spirit of Refs. 33 and 37, we regard as the ''FR state'' the oxygen contribution to the Pr $4f_{z(x^2-y^2)}-(\alpha_1|\mathrm{O}\ 2p_x\rangle+\alpha_2|\mathrm{O}\ 2p_y\rangle+\alpha_3|\mathrm{O}\ 2p_z\rangle)$ hybridization. In Ref. 33, the coefficients α_1, α_2, and α_3 are chosen in such a way that the O $2p_\pi$ hybrids which are σ bonded to the Pr $4f_{z(x^2-y^2)}$ state have an out-of-plane character equal in magnitude to their in-plane character. This can be visualized by a 45° ''rotation angle'' of the O $2p_\pi$ hybrids toward the plane, and it is in this sense that we will be using the expression ''rotation angle'' throughout this paper. By the same token, the FR state as proposed in Ref. 33, i.e., with a rotation angle of 45°, will be referred to as an ''isotropic'' FR state.

[35] F. C. Zhang and T. M. Rice, Phys. Rev. B **37**, 3759 (1987).

[36] Magnetic interactions have been thought to be responsible for splitting off the so-called Zhang-Rice singlet from the valence band in the following way: Strong hybridization between Cu $3d_{x^2-y^2}$ and O $2p_{x,y}$ orbitals leads to interaction of the spin of an intrinsic hole on a Cu(2) site and the spin of a doped hole on the four surrounding O(2,3) sites. For antiparallel spin orientation, the Zhang-Rice singlet is pushed out of the valence band. Since this is a widespread interpretation, we will adopt the notation ''ZR state'' for the uppermost part of the valence band although our experiments cannot provide any insight into its magnetic interaction.

[37] A. I. Liechtenstein and I. I. Mazin, Phys. Rev. Lett. **74**, 1000 (1995).

[38] Y. Wang, H. Rushan, and Z.-B. Su, Phys. Rev. B **50**, 10 350 (1994).

[39] D. Khomskii, J. Supercond. **6**, 69 (1993).

[40] H. A. Blackstead and J. D. Dow, Phys. Rev. B **51**, 11 830 (1995).

[41] A. Erb, T. Biernath, and G. Müller-Vogt, J. Cryst. Growth **132**, 389 (1993); A. Erb, T. Traulsen, and G. Müller-Vogt, *ibid.* **137**, 487 (1994).

[42] A. Erb, E. Walker, and R. Flükiger, Physica C **245**, 245 (1995); **258**, 9 (1996).

[43] K. Widder and H. P. Geserich (private communication).

[44] A. Zibold, M. Dürrler, H. P. Geserich, A. Erb, and G. Müller-Vogt, Physica C **171**, 151 (1990).

[45] Laboratoire commun CEA-CNRS.

[46] P. Schweiss, W. Reichardt, M. Braden, G. Collin, G. Heger, H. Claus, and A. Erb, Phys. Rev. B **49**, 1387 (1994).

[47] U. H. Zucker, E. Perenthaler, W. F. Kuhs, R. Bachmann, and H. Schulz, J. Appl. Crystallogr. **16**, 358 (1983).

[48] We note that an inspection of the Pr $M_{\mathrm{IV,V}}$ edges cannot add any further information or significance to O K results: (a) The interference of the Pr M_{IV} and M_{V} edges with the Cu L_{II} and L_{III} edges, respectively, renders a deconvolution of these structures impossible. (b) Even without this interference a cross-examination of the O K results would not be reliable since the Pr M features correspond to 12 holes in the f shell of Pr^{3+}, not to just about one as for the O K edge. The amount of, say, 0.2 holes added to or removed from the edge structure constitutes a substantial fraction of the O K edge while it is a mere 2% effect for the Pr M features.

[49] L. Tröger, D. Arvanitis, K. Baberschke, H. Michaelis, U. Grimm, and E. Zschech, Phys. Rev. B **46**, 3283 (1992).

[50] S. Eisebitt, T. Böske, J.-E. Rubensson, and W. Eberhardt, Phys. Rev. B **47**, 14 103 (1993).

[51] J. J. Yeh and I. Lindau, At. Data Nucl. Data Tables **32**, 1 (1985).

[52] W. J. Veigele, *Handbook of Spectroscopy* (CRC Press, Cleveland, 1974), Vol. 1, p. 28.

[53] O. Cohen, F. H. Potter, C. S. Rastomjee, and R. G. Egdell, Physica C **201**, 58 (1992).

[54] N. Nücker, H. Romberg, X. X. Xi, J. Fink, B. Gegenheimer, and Z. X. Zhao, Phys. Rev. B **39**, 6619 (1989).

[55] W. E. Pickett, Rev. Mod. Phys. **61**, 433 (1989).

[56] J. Zaanen, M. Aluani, and O. Jepsen, Phys. Rev. B **40**, 837 (1989).

[57] W. Y. Ching, G.-L. Zhao, Y.-N. Xu, and K. W. Wong, Phys. Rev. B **43**, 6159 (1991).

[58] N. Nücker, E. Pellegrin, P. Schweiss, J. Fink, S. L. Molodtsov, C. T. Simmons, G. Kaindl, W. Frentrup, A. Erb, and G. Müller-Vogt, Phys. Rev. B **51**, 8529 (1995).

[59] A. Hartmann and G. J. Russell, Solid State Commun. **95**, 791 (1995); **90**, 745 (1994); **89**, 77 (1994).

[60] H. Eskes, M. B. Meinders, and G. A. Sawatzky, Phys. Rev. Lett. **67**, 1035 (1991).

[61] M. B. Meinders, H. Eskes, and G. A. Sawatzky, Phys. Rev. B **48**, 3916 (1993).

[62] K. Widder, M. Merz, D. Berner, J. Münzel, H. P. Geserich, A. Erb, R. Flükiger, W. Widder, and H. F. Braun, Physica C **264**, 11 (1996).

[63] Y. H. Ko, H. K. Kweon, H. C. Lee, and N. H. Hur, Physica C **224**, 357 (1994).

[64] H. Lütgemeier and I. Heinmaa, in *Proceedings of the 26th Zakopane Summer School on Physics*, edited by J. Stanek and A. T. Pędziwiatr (World Scientific, Singapore, 1991), p. 264.